

# Memory Requirements to Mitigate Fading Losses on an Optical Channel

B. Moision<sup>1</sup> and A. Biswas<sup>1</sup>

*A deep-space optical communications channel is subject to fading losses due to pointing and tracking errors. Barron and Boroson [1] illustrated that these losses may be mitigated by introducing an interleaver that spreads a pointing-induced fade over many codewords of an error-correction code. Several approximations to determine the interleaver gain, which can be computationally prohibitive, are introduced in [1]. However, the methods are accurate only for a range of code rates and interleaver depths. We extend these methods, using a nonlinear fit to capacity, to allow the analysis of any code rate and fading depth. We also develop an efficient and accurate approximation of the finite-interleaving losses by an inversion of the Marcum Q-function, and provide expressions relating the interleaver memory to the finite-interleaver losses. The resulting expressions provide an accurate tool for a system engineer to size the interleaver memory as a function of the data rate and the allowable pointing loss.*

## I. Introduction

NASA's pursuit of the vision for space exploration [2] requires orders of magnitude increases in data return rates from planetary distances. An optical communications link transmitting a narrow laser beam from planetary distances holds great promise for delivering the increased data rates while imposing reasonable mass and power burdens on a host spacecraft [3]. To realize the benefits of deep-space optical communications will require accurate and reliable beam pointing to limit pointing losses that would otherwise prevent link closure. Pointing accuracies of 0.1 to 0.2 of the transmitted beam width are typically sufficient [4]. This beam pointing must be implemented in the presence of vibrational disturbances, spacecraft attitude fluctuations, and (longer-term) thermal drifts. Strategies for beam-pointing control against the wide spectrum of disturbances are well established for near-Earth space platforms. While preliminary designs exist for deep-space applications, pointing control is still an active area of study.

In [1], Barron and Boroson investigate the mitigation of pointing losses by introducing an interleaver/deinterleaver in the signaling chain. An interleaver spreads out a pointing-induced fade over many codewords of the error-correction code (ECC), allowing the fade to be corrected and limiting pointing losses. In the example in [1], with parameters drawn from models of the since discontinued Mars Laser Communications Demonstration (MLCD), the introduction of a modest-sized interleaver reduced the

---

<sup>1</sup> Communications Architectures and Research Section.

The research described in this publication was carried out by the Jet Propulsion Laboratory, California Institute of Technology, under a contract with the National Aeronautics and Space Administration.

pointing loss by 1.8 dB. This gain was achieved by signal processing alone, with no improvements to the mechanical pointing system. In general, the gain will depend upon the coherence time, fading depth, and the interleaver depth.

The theoretical limit on performance of the channel is given by the fading channel capacity. The fading channel capacity is the least upper bound on the throughput with no latency constraints, in particular, allowing an infinite interleaver. Losses are accrued when imposing a latency constraint that limits the size of the interleaver. These losses are well characterized by the outage probability. However, a straightforward computation of the outage probability would be prohibitively time consuming. Several methods to alleviate the computational complexity are developed in [1]. The first, based on a linear model of capacity, is accurate for ECC rates around 1/2 and fading depths of 1 to 2 dB. The second, a Gaussian approximation, is accurate for large diversity and small outage probabilities.

In this article, we extend the results from [1], providing a nonlinear approximation to capacity that is accurate over the entire domain, developing an efficient and accurate approximation of the finite-interleaving losses by an inversion of the Marcum Q-function, and providing expressions relating the interleaver memory to the finite-interleaver losses. The goal is to provide a system engineer with an accurate tool for sizing the interleaver memory as a function of the data rate and the allowable pointing loss.

This article is organized as follows. Section II describes the fading channel model. In Section III, we define the capacity of the channel and give some linear and nonlinear approximations for the capacity. Section IV discusses the outage probability and approximations to it. Section V describes interleavers required to effectively disperse a fade, and Section VI combines the results, mapping fading losses to a memory requirement.

## II. Fading Channel Model

We adopt the fading channel model from [1], which is briefly reviewed in this section. Pointing and tracking loops at the transmitter and receiver attempt to orient a detector relative to the transmitted beam to maximize the received intensity. The transmitted information-bearing signal is pulse-position-modulated (PPM) and received over a Poisson channel, with  $M$  the PPM order and  $n_b$  the mean noise photons per slot (note that the noise is not affected by tracking errors). With perfect tracking, an average  $n_s$  photons are received per pulsed slot, and an average  $P_{av} = n_s/M$  photons are received per slot. To simplify notation, we refer to  $P_{av}$  as the average power, in photons/second, as opposed to  $P_{av}h\nu/T_s$ , in watts, where  $h$  is Planck's constant,  $\nu$  the frequency, and  $T_s$  the slot width.

Let  $w(t) = (w_x(t), w_y(t))$  be the two-dimensional (2-D) tracking error at time  $t$ , where  $w_x, w_y$  are orthogonal directions of angular displacement. The beam intensity is Gaussian as a function of the angular displacement, yielding an instantaneous fade of

$$v(t) = \exp\left(-\frac{w_x(t)^2 + w_y(t)^2}{2\sigma_b^2}\right)$$

where  $\sigma_b$  is the angular beam width. The intensity is presumed constant during a slot, so that the mean signal photons per pulsed slot in the presence of fading is  $vn_s$ , where  $v$  is a sample of the process  $v(t)$ . To simplify notation, we let  $\sigma_b = 1$  and use units of beam widths for angular displacement throughout. Since the beam is symmetric, we may assume without loss of generality that the mean tracking error is entirely in the x-direction. The tracking error is modeled as a circularly symmetric Gaussian random process with marginal variance  $\sigma^2$  and a mean pointing error of  $m$ , i.e.,  $w(t)$  is distributed as  $\mathcal{N}([m, 0], \sigma^2 I)$ . This yields a mean signal power in the presence of fading of

$$P_{av}E[v(w)] = P_{av} \frac{1}{1 + \sigma^2} \exp\left(\frac{-m^2}{2(1 + \sigma^2)}\right)$$

This represents a static loss of received power that cannot be recovered.

We assume throughout that the decoder has perfect knowledge of the intensity. This is a reasonable assumption since the coherence time of the fading time series is typically much longer than the slot, or sampling, time and may be estimated accurately. Moreover, the loss relative to having no such information for a typical Mars–Earth link has been shown to be less than 0.1 dB.<sup>2</sup>

The coherence time,  $T_{coh}$ , of the pointing error, or fading, process is the minimum duration such that samples of the fading process separated by more than  $T_{coh}$  are (approximately) uncorrelated. For example, a coherence time of  $T_{coh} = 20$  ms is typical for recent pointing budgets proposed for an Earth–Mars link [1]. We assume a block-fading model of the pointing error, i.e., that the fading process  $v(t)$  takes a fixed value over one coherence interval, drawn from the distribution on  $v$ , then takes a fixed value in the next coherence interval, drawn independently from the distribution on  $v$ , and so on.

The sequence of transmitted PPM symbols is interleaved prior to transmission, and received symbols are deinterleaved on reception. A codeword consists of  $N_{cw}$  PPM symbols, which may have seen different fades, depending on the interleaver depth and coherence time. Let  $N_f$  be the number of independent fade realizations per codeword. We assume that these fades are distributed equally throughout the codeword, i.e., that there are  $N_f$  groups of  $Z$  symbols with  $N_{cw} \approx N_f Z$ , as would approximately be the case for a well-designed interleaver.

### III. Channel Capacity

We will assume throughout that  $M$  and  $n_b$  are fixed, and express performance as a function of the average power. Unless otherwise noted, capacity is expressed in units of bits/slot. The fundamental limitation on the throughput that can be achieved on the fading channel is the fading capacity given by

$$\begin{aligned} C_{fad}(P_{av}) &= \int_0^\infty C(vP_{av})f_v(v)dv \\ &= E_v[C(vP_{av})] \end{aligned}$$

where  $C(P_{av})$  is the capacity of the unfaded channel with average power  $P_{av}$  and  $f_v$  is the density function of the fading process.

We also refer to the “power in decibels such that the capacity equals rate  $R$ ” as

$$P_{cap,fad,dB}(R) = \{10 \log_{10} P_{av} : C_{fad}(P_{av}) = R\}$$

This represents the minimum power required to close the link, i.e., to achieve arbitrarily small probability of error, with a code of rate  $R$ . For the Poisson PPM channel, the capacity is given by [5]

---

<sup>2</sup>R. Barron, “Quantifying the Effects of Channel Interleaving on MLCD System Performance in a Fading Environment,” Technical Report, MIT Lincoln Laboratory, Lexington, Massachusetts, June 2004.

$$C(P_{av}) = \begin{cases} \frac{\log_2 M}{M} \left( 1 - \frac{1}{\log_2 M} E_{y_1, \dots, y_M} \log_2 \left[ \sum_{j=1}^M \left( 1 + \frac{MP_{av}}{n_b} \right)^{(y_j - y_1)} \right] \right), & n_b > 0 \\ \frac{\log_2 M}{M} (1 - e^{-n_s}), & n_b = 0 \end{cases} \quad (1)$$

where  $y_1$  is Poisson with mean  $n_b + n_s$  and the  $y_j, j = 2, \dots, M$  are Poisson with mean  $n_b$ . Equation (1) may be evaluated accurately via a sample mean. However, this can be inefficient and does not lend itself to analytical approximations. The following sections present approximations to Eq. (1).

### A. Linear Approximation

Figure 1 illustrates  $C(P_{av})$  for  $M = 64$  parameterized by  $n_b$ .  $C(P_{av})$  is approximately linear in  $\log P_{av}$  in a region around  $\log_2 M/(2M)$ —the region corresponding to a rate 1/2 code. It was noted in [1] that the capacity in this region may be well approximated as

$$C(P_{av}) \approx a \log(P_{av}) + \gamma \quad (2)$$

where  $a, \gamma$  are functions of  $M, n_b$ . Linear fits to  $C(P_{av})$  are illustrated in Fig. 1. Intercepts for ECC rates of 1/4, 1/2, and 7/8 are also illustrated (corresponding to composite rates of (ECC Rate)  $\times \log_2 M/M$  bits/slot). Applying the linear approximation gives an approximation to the threshold [1]:

$$P_{cap, fad, dB} \approx 10 \log_{10}(e) \left( \frac{R - \gamma}{a} + \sigma^2 + \frac{m^2}{2} \right) \quad (3)$$

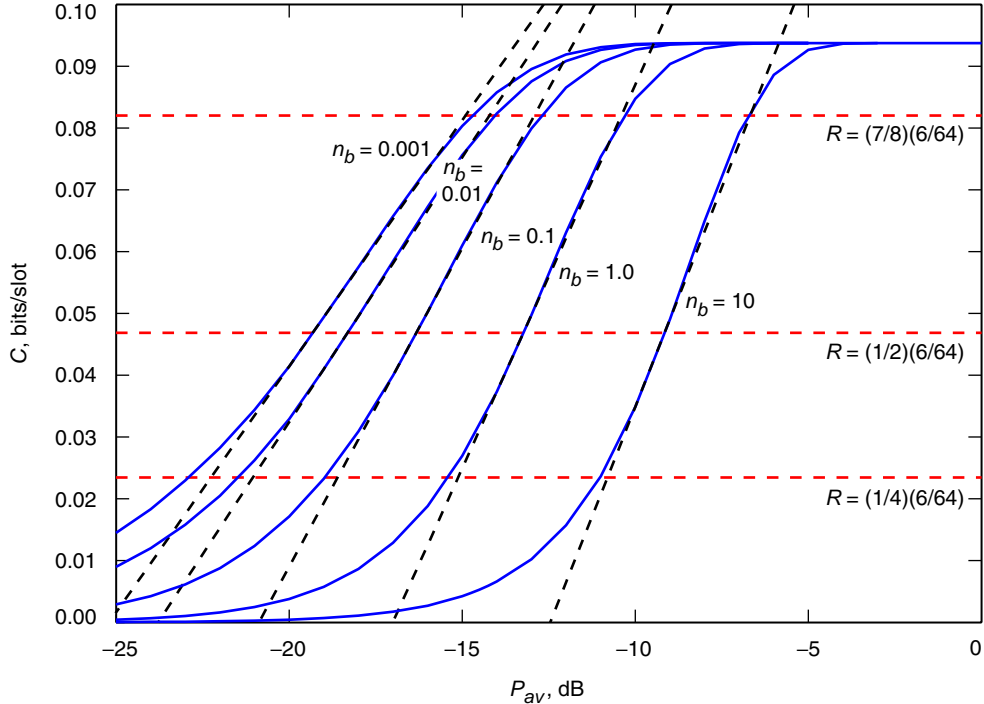


Fig. 1. PPM capacity,  $M = 64$ , and linear approximations.

## B. Nonlinear Approximation

As illustrated in Fig. 1, the linear fit is accurate in an  $\approx \pm 2$  dB range of  $P_{av}$  around the intercept for an ECC rate of  $1/2$ . If the ECC rate differs significantly from  $1/2$  (or the depths of fades are significantly greater than 2 dB), the linear fit will yield inaccurate results. In order to evaluate the capacity efficiently outside the region where the linear approximation holds, we developed the following nonlinear fit to capacity:

$$C(P_{av}) \approx \begin{cases} \frac{(n_s + n_b) \log(1 + n_s/n_b) - n_s}{\log(2)}, & P_{av} \leq P_{av}^{(1)} \\ \sum_{i=0}^4 \alpha_i P_{av}^i, & P_{av}^{(1)} < P_{av} \leq P_{av}^{(2)} \\ \beta_0 - \exp\left(\sum_{i=1}^4 \beta_i P_{av}^{(i-1)}\right), & P_{av}^{(2)} < P_{av} \leq P_{av}^{(3)} \\ \frac{\log_2 M}{M}, & P_{av} > P_{av}^{(3)} \end{cases}$$

The estimates for high and low  $P_{av}$  are asymptotically tight as  $P_{av}$  goes to infinity and zero, respectively. The remaining domain is split into a region where a polynomial fit is tight and one where an exponential fit is tight. The coefficients may be determined from the Levenberg–Marquand algorithm [6]. Table 1 lists a set of coefficients for  $M = 64, n_b = 0.2$ . Figure 2 illustrates errors in the four approximations relative to an evaluation of the sample mean with at least  $10^7$  samples, as well as the linear fit, showing the regions where the four approximations are tight. Residual errors on the order of hundredths of a decibel are due to uncertainty in the “true” value, which is itself an approximation by means of the sample mean.

## IV. Probability of Outage

To approach the fading channel capacity requires codewords of increasing duration. Codeword lengths and interleaving depths in practice are limited by latency and memory constraints. We would like a measure of the capacity under a finite codeword or interleaver constraint in order to predict losses and design interleavers. One approach would be to define the capacity for a channel with finite codewords as the minimum required power such that information may be transmitted with an arbitrarily small probability of error. This is, however, a misleading quantity on a fading channel, since there will be a finite probability that every symbol in the codeword sees the worst-case fading. This definition of capacity will be dominated by the worst-case fading, which can be significantly worse than the degradation measured at a required error rate.

**Table 1. Coefficients for fitting PPM capacity,  $M = 64, n_b = 0.2$ ,  
 $P_{av}^{(1)} = -22.5$  dB,  $P_{av}^{(2)} = -15.0$  dB,  $P_{av}^{(3)} = -7.5$  dB.**

$i$	$\alpha_i$	$\beta_i$
0	$1.289 \times 10^{-3}$	0.09375
1	0.5937	-2.322
2	98.17	-16.47
3	$-2.687 \times 10^3$	-383.9
4	$2.199 \times 10^4$	$1.462 \times 10^3$

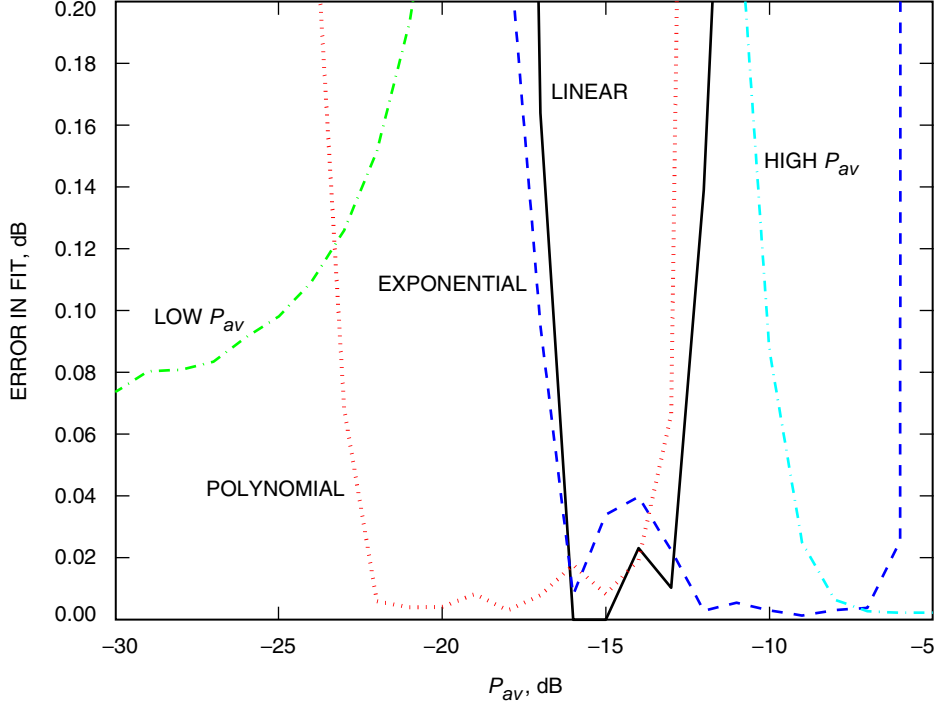


Fig. 2. Tightness of fits to PPM capacity,  $M = 64$ ,  $n_b = 0.2$ .

A more accurate representation of the degradation is given by the probability of outage,

$$\begin{aligned}
 p_{out}(R, P_{av}) &= Pr(\bar{C} \leq R) \\
 &= \int_0^R f_{\bar{C}}(c) dc
 \end{aligned} \tag{4}$$

the probability that the instantaneous capacity  $\bar{C}$  falls below the rate of the code, where the instantaneous capacity of an  $N_f$ -block fading channel is given by

$$\bar{C} = \frac{1}{N_f} \sum_{i=1}^{N_f} C(v_i P_{av}) \tag{5}$$

where the  $v_i$  are independent samples of the process  $v$ . As  $N_f \rightarrow \infty$ , the instantaneous capacity approaches the fading capacity and the outage probability approaches a step function.

Inverting Eq. (4) yields  $P_{av,dB}(R, p_{out}^*, N_f) = \{10 \log_{10} P_{av} : p_{out}(R, P_{av}) = p_{out}^*\}$ , the average power required to achieve outage probability  $p_{out}^*$  for a given interleaving depth  $N_f$ . The difference

$$\text{loss}_{dB} = P_{av,dB}(R, p_{out}, N_f) - P_{cap,fad,dB}(R)$$

represents the finite interleaving loss—the power required in addition to the fading capacity to achieve a specified outage probability. In the remainder of this section, we discuss several methods to compute or estimate  $p_{out}$ .

### A. Monte Carlo Estimation, Nonlinear Approximation

Determining  $f_{\bar{C}}$  accurately can be problematic; hence, rather than evaluate Eq. (4) by estimating  $f_{\bar{C}}$ , we may compute an estimate of  $p_{out}(R, P_{av})$  by means of Monte Carlo simulation. A sample of  $\bar{C}$  is generated by first generating  $N_f$  samples  $v_1, \dots, v_{N_f}$  and computing  $C(v_i P_{av})$ . An estimate of each  $C(v_i, P_{av})$  may be generated by a sample mean or by the nonlinear approximations developed earlier. For example, Fig. 3 illustrates the outage probability computed using the nonlinear approximation for the case  $R = 1/4, M = 64, n_b = 0.2, m = 0.25, \sigma = 0.2$ , and varying interleaving depths. Losses of 2.75 dB with no interleaving can be reduced to less than 0.15 dB with sufficient interleaving.

### B. Linear Approximation

Approximation (2) leads to the following closed form for  $p_{out}$  [1]:

$$p_{out}(R, P_{av}) \approx Q_{N_f} \left( \frac{\sqrt{N_f} m}{\sigma}, \frac{\sqrt{2N_f}(\gamma + a \log P_{av} - R)/a}{\sigma} \right) \quad (6)$$

where

$$Q_m(\alpha, \beta) = \int_{\beta}^{\infty} x \left( \frac{x}{\alpha} \right)^{n-1} \exp(x^2 + \alpha^2) I_{n-1}(\alpha x) dx$$

is the generalized Marcum Q-function. In numerical results, we evaluate the Marcum Q-function by means of the recursive algorithms presented in [7].

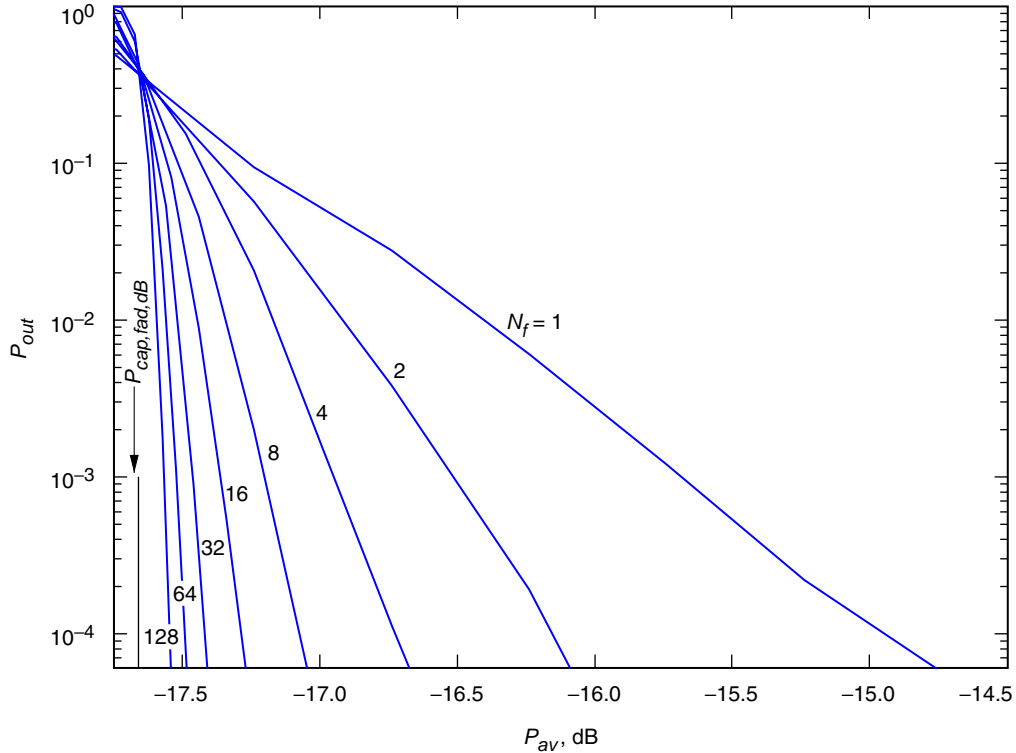


**Fig. 3. Outage probability parameterized by interleaving depth  $N_f$ .**

$R = 1/4, M = 64, n_b = 0.2, m = 0.25, \sigma = 0.2.$

Solving Approximation (6) for  $P_{av}$  is, in general, problematic. However, models of tracking errors show that  $m$  and  $\sigma$  vary such that their ratio remains relatively constant. This motivates the following inversion of Approximation (6), extending the results from [1]. Let  $Q_{N_f}^{-1}(p_{out}; m/\sigma) = \{\xi | Q_{N_f}(\sqrt{N_f}m/\sigma, \sqrt{N_f}\xi) = p_{out}\}$ , which may be precomputed for integer  $N_f$  and a fixed ratio  $m/\sigma$ . This gives an approximation for the average power,

$$P_{av,dB} \approx 10 \log_{10}(e) \left( \left( Q_{N_f}^{-1} \left( p_{out}; \frac{m}{\sigma} \right) \right)^2 \frac{\sigma^2}{2} + \frac{R - \gamma}{a} \right)$$

Taking the difference with Approximation (3) yields

$$\text{loss}_{dB} \approx 5 \log_{10}(e) \sigma^2 \left( Q_{N_f}^{-1} \left( p_{out}; \frac{m}{\sigma} \right)^2 - \left( 2 + \left( \frac{m}{\sigma} \right)^2 \right) \right) \quad (7)$$

The loss is not a function of the rate, PPM order, or the noise.

### C. Gaussian Approximation

For large  $N_f$ ,  $\bar{C}$  may be approximated as Gaussian with mean  $\mu_{\bar{C}} = \mu_C = E[C(\mathbf{v}P_{av})] = C_{fad}$  and variance  $\sigma_{\bar{C}}^2 = \text{var}(C(\mathbf{v}P_{av}))/N_f = \sigma_C^2/N_f$ . Under a Gaussian approximation, the outage probability is given by [1]

$$p_{out}(R, P_{av}) \approx \frac{1}{2} \text{erfc} \left( \frac{\sqrt{N_f}(\mu_C - R)}{\sigma_C \sqrt{2}} \right) \quad (8)$$

Applying Approximation (2), we may approximate the mean and variance as

$$\mu_C \approx a \log P_{av} + \gamma - a \left( \sigma^2 + \frac{m^2}{2} \right) \quad (9)$$

$$\sigma_C^2 \approx \frac{a^2}{2} (m^2 \sigma^2 + \sigma^4) \quad (10)$$

Substituting Approximations (9) and (10) into Approximation (8) and inverting yields

$$P_{av,dB} \approx 10 \log_{10}(e) \left( \sqrt{\frac{\sigma^2 + m^2 \sigma^2}{2N_f}} \text{erfc}^{-1}(2p_{out}) + \frac{R - \gamma}{a} + \left( \sigma^2 + \frac{m^2}{2} \right) \right) \quad (11)$$

Taking the difference with Approximation (3) yields an approximation of the finite interleaver loss,

$$\text{loss}_{dB} \approx 10 \log_{10}(e) \sqrt{\frac{\sigma^2 + m^2 \sigma^2}{2N_f}} \text{erfc}^{-1}(2p_{out}) \quad (12)$$



## D. Approximation Accuracy

Figure 4 illustrates five estimates of  $p_{out}$  for the case  $N_f = 4, M = 64, n_b = 0.2, m = 0.2, \sigma = 0.25, R = (1/4)(6/64)$ : from Monte Carlo simulation where  $C(v_i P_{av})$  is computed by means of a sample mean; from Monte Carlo simulation where  $C(v_i P_{av})$  is determined from the nonlinear approximation; by means of the Linear Approximation (6); by means of the Gaussian Approximation (8) with estimated mean and variance; and by means of the Gaussian Approximation (8) with mean and variance from Linear Approximations (9) and (10). In this region, the linear approximation underestimates the mean and overestimates the variance. The Gaussian approximation using a sample mean and variance is good, even with such small  $N_f$ . However, the Gaussian and linear approximations lead to an underestimate of  $\text{loss}_{dB}$  by means of Approximation (12). We see no difference between the nonlinear approximation and Monte Carlo simulations.

## V. Interleavers

In this section, we give relationships between the size of an interleaver, measured in bits, and the resulting spread, measured in independent fades per codeword,  $N_f$ . Interleaving in all cases will be over PPM symbols. This imposes no loss relative to interleaving over slots, since each symbol has only one slot affected by fading (noise slots are not affected). Let  $N_b$  be the interleaver memory size in bytes. We assume there are  $M$  bytes per soft symbol at the receiver—one byte per slot. We have found this is sufficient to yield negligible performance degradation in a soft-decision decoding algorithm [8]. Results may be scaled to reflect changes to the bits/symbol quantization. Let  $N_{coh} = T_{coh}/T_{symbol}$ , the duration of the coherence time in symbols, and recall  $N_{cw} = T_{codeword}/T_{symbol}$ , the duration of a codeword in symbols.

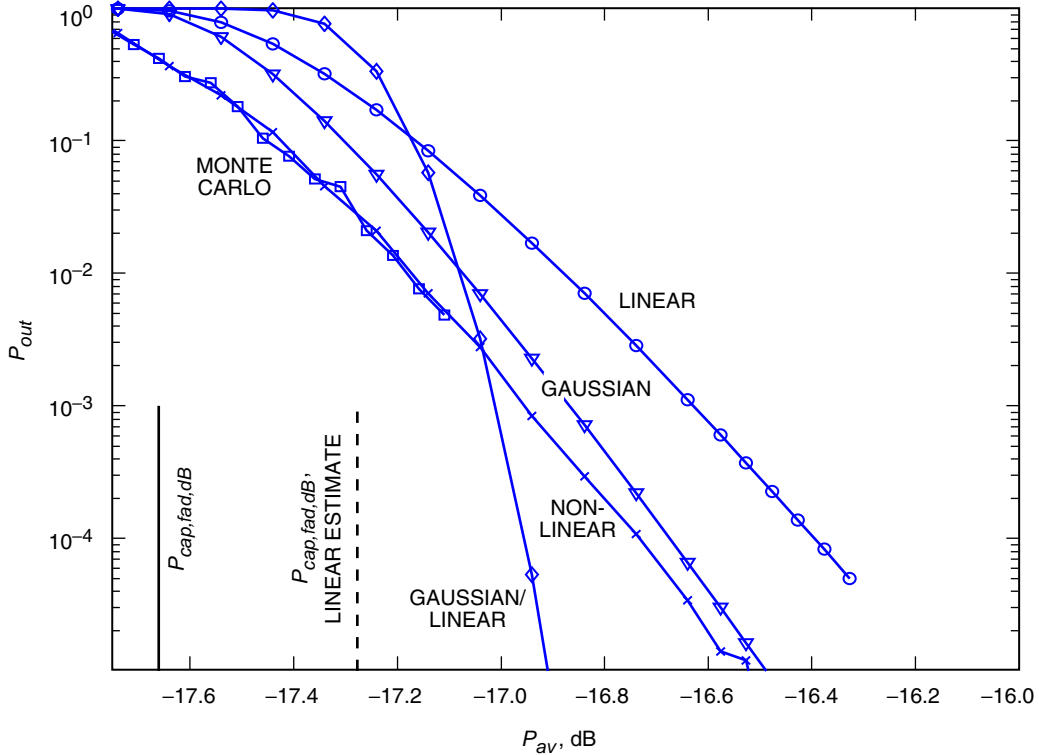


**Fig. 4. Approximations to the outage probability,**  
 $M = 64, \sigma = 0.25, m = 0.2, n_b = 0.2$ .

### A. Block Interleaver

A block interleaver writes received symbols to a  $P \times Q$  matrix in rows and reads them out in columns. The memory required is  $N_b = MPQ$  bytes. Suppose  $PQ > N_{cw}$ . A spreading of  $N_f$  is achieved by choosing  $P = N_f, Q = N_{coh}$ , such that

$$N_f = \frac{N_b}{MN_{coh}}$$

### B. Convolutional Interleaver

A convolutional interleaver, illustrated in Fig. 5, consists of  $N$  rows of delays (shift registers) of length  $0, B, 2B, \dots, (N-1)B$ , where each register contains one PPM symbol. The memory required for the interleaver is  $N_b = M \times N(N-1)B/2$  bytes. For an input sequence  $\dots, v_0, v_1, \dots$ , where each  $v_i$  is the faded amplitude of a symbol, i.e., of the signal slot in that symbol, the interleaver output is

$$\dots, v_{kN}, v_{(k-B)N+1}, v_{(k-2B)N+2}, \dots, v_{(k-(N-1)B)N+N-1}, v_{(k+1)N}, \dots$$

We see that adjacent symbols in the output correspond to input symbols separated by  $NB-1$  or  $NB(N-1)+1$ . Similarly, adjacent symbols in the input, e.g.,  $v_0, v_1$ , are separated in the output by  $NB-1$  or  $NB(N-1)+1$  symbols (the interleaver is symmetric in this sense). Suppose  $N$  divides  $N_{cw}$  and the first bit of the codeword corresponds to  $v_{kN}$ . Then the block of symbols corresponding to a single codeword spans a duration of

$$\begin{aligned} kN - \left( \left( k - \frac{N_{cw}}{N} - 1 - (N-1)B \right) N + N - 1 \right) &= N(N-1)B + N_{cw} + 1 \text{ symbols} \\ &\approx N(N-1)B \text{ symbols} \end{aligned}$$

and, hence,

$$\begin{aligned} N_f &\approx \frac{N(N-1)B}{N_{coh}} \\ &= \frac{2N_b T_s}{T_{coh}} \end{aligned} \tag{13}$$

and we see that a convolutional interleaver achieves twice the diversity of a block interleaver with the same memory. In the remainder, we assume a convolutional interleaver is used and use Eq. (13) to relate the memory and spreading achieved by the interleaver.

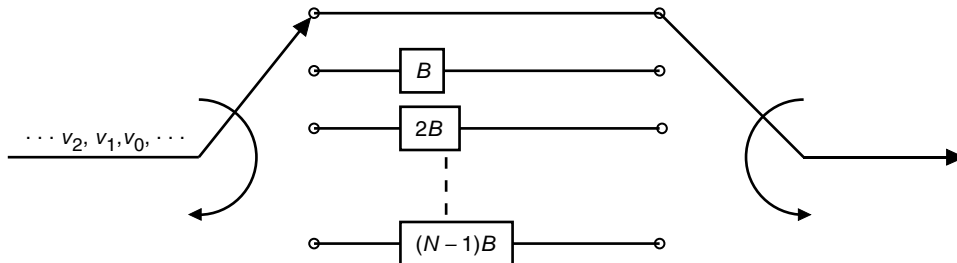


Fig. 5. A convolutional interleaver.

## VI. Memory Requirements

Figure 6 illustrates  $\text{loss}_{dB}$  as a function of the interleaver depth  $N_f$  with  $p_{out} = 10^{-4}$ ,  $m = 0.2$ , and  $\sigma = 0.25$ . Illustrated are a computation using the nonlinear approximation for  $C(v_i P_{av})$ , the Linear Approximation (7), and the Gaussian/Linear Approximation (12). The linear approximation is very accurate since, as illustrated in Fig. 4, errors in  $P_{av,dB}$  and  $P_{cap,fad,dB}$  offset.

The interleaving depth may be mapped to a memory requirement by means of Eq. (13). For example, to reduce losses to less than 0.2 dB requires  $N_f \approx 64$ . This can be achieved on a channel with a coherence time of  $T_{coh} = 10$  ms and slot widths of  $T_s = 1$  ns with an interleaver of

$$N_b = \frac{N_f T_{coh}}{2T_s} = 40 \text{ Mbytes}$$

An approximation of the memory requirements to limit losses to less than  $\text{loss}_{dB}$  may be obtained by applying the Gaussian/linear approximation. Solving Approximation (11) for  $N_f$  yields

$$N_b \approx \left\lceil \frac{(10 \log_{10}(e) \operatorname{erfc}^{-1}(2p_{out}))^2 (\sigma^4 + m^2 \sigma^2)}{\text{loss}_{dB}^2} \right\rceil \frac{T_{coh}}{2T_s}$$

We see that the memory requirements are inversely quadratic in the required decibel loss.

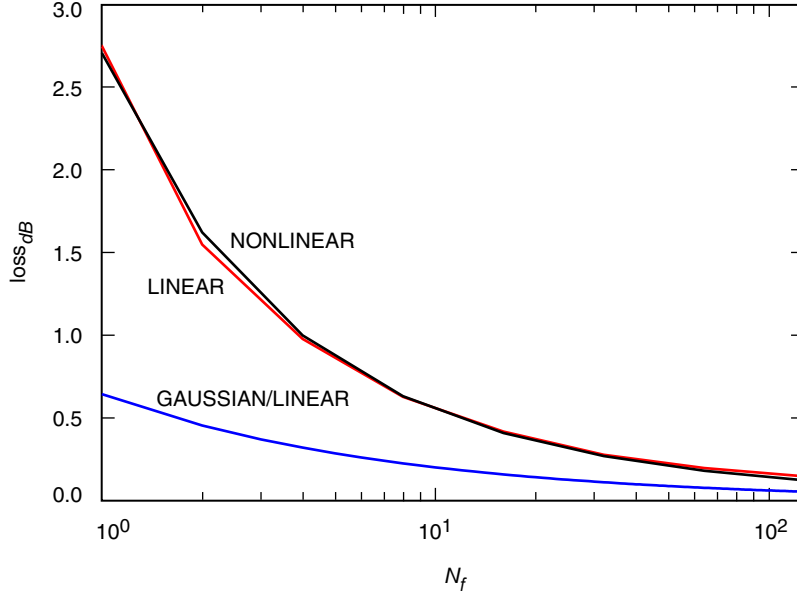


**Fig. 6. Fading loss (relative to fading capacity) as a function of interleaver memory,  $m = 0.20$ ,  $\sigma = 0.25$ .**

## VII. Conclusions

In this article, we have extended methods to compute the losses due to fading on an optical channel. To determine the capacity efficiently in regions where a linear approximation is inaccurate, a presented nonlinear approximation may be used. However, the nonlinear approximations, although very accurate, do not lend themselves to closed-form solutions to the finite interleaver losses. The errors from the linear approximation of the fading channel capacity and the outage probability offset to yield an accurate estimate of the finite interleaver loss. Gaussian approximations remain accurate only if accurate estimates of the mean and variance are used.

Desired finite interleaver losses may be mapped to memory requirements in a straightforward manner. This allows a system designer to see the cost (in memory) of combating fading—e.g., to determine how much storage is required to limit losses to some acceptable quantity.

## References

- [1] R. J. Barron and D. M. Boroson, “Analysis of Capacity and Probability of Outage for Free-Space Optical Channels with Fading due to Pointing and Tracking Error,” *Proceedings of the SPIE*, G. S. Mecherle, ed., vol. 6105, 12 pp., March 2006.
- [2] “NASA’s Vision for Space Exploration,” NASA Web site, [www.nasa.gov/pdf/55583main-vision-space-exploration2.pdf](http://www.nasa.gov/pdf/55583main-vision-space-exploration2.pdf).
- [3] W. D. Williams, M. Collins, D. M. Boroson, J. Lesh, and A. Biswas, “RF and Optical Communications: A Comparison of High Data Rate Returns from Deep Space in the 2020 Timeframe,” *Proceedings of the 12th Ka and Broadband Communications Conference*, Naples, Italy, 15 pp., September 2006.
- [4] V. W. S. Chan, “Optical Space Communications,” *IEEE Journal of Selected Topics in Quantum Electronics*, vol. 6, pp. 959–975, November/December 2000.
- [5] B. Moision and J. Hamkins, “Deep-Space Optical Communications Downlink Budget: Modulation and Coding,” *The Interplanetary Network Progress Report 42-154, April–June 2003*, Jet Propulsion Laboratory, Pasadena, California, pp. 1–28, August 15, 2003. [http://ipnpr/progress\\_report/42-154/154K.pdf](http://ipnpr/progress_report/42-154/154K.pdf)
- [6] W. H. Press, S. A. Teukolsky, W. T. Vetterling, and B. P. Flannery, *Numerical Recipes in C*, second ed., New York: Cambridge University Press, 1992.
- [7] C. W. Helstrom, *Elements of Signal Detection and Estimation*, Englewood Cliffs, New Jersey: Prentice Hall, 1995.
- [8] M. K. Cheng, M. A. Nakashima, J. Hamkins, B. E. Moision, and M. Barsoum, “A Field-Programmable Gate Array Implementation of the Serially Concatenated Pulse-Position Modulation Decoder,” *The Interplanetary Network Progress Report*, vol. 42-161, Jet Propulsion Laboratory, Pasadena, California, pp. 1–14, May 15, 2005. [http://ipnpr/progress\\_report/42-161/161S.pdf](http://ipnpr/progress_report/42-161/161S.pdf)